

The Radius of Neutron Stars



Bob Rutledge
McGill University

Collaborators: **Sebastien Guillot (McGill)**. Mathieu Servillat (Saclay) Natalie Webb (Toulouse). Ed Brown (MSU) Lars Bildsten (UCSB/KITP) George Pavlov (PSU) Vyacheslav Zavlin (MSFC).

Theoretical
Unified Force

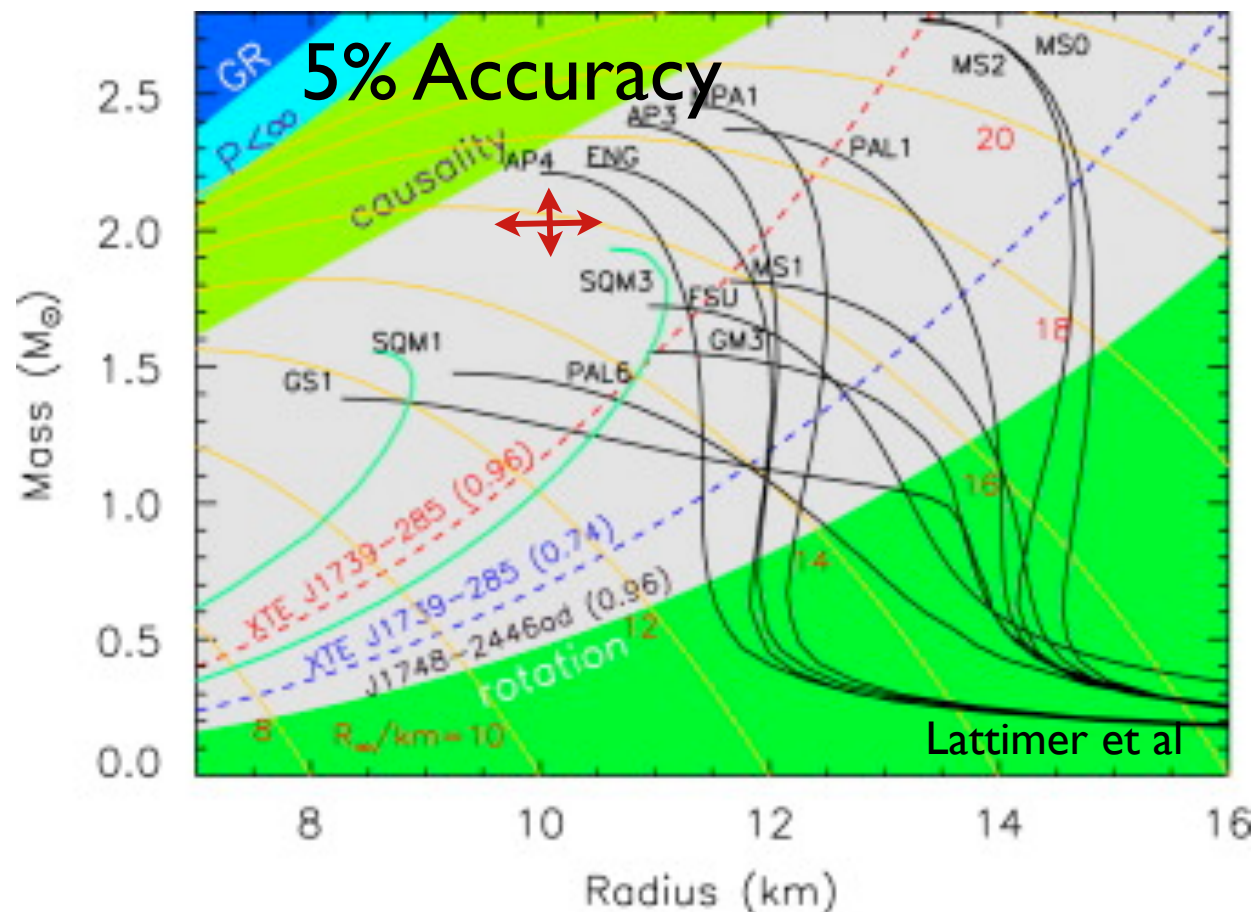
A physicist, in 2013, cannot solve equations which permit an analytic prediction from the physics of the strong force regarding the systems where this force is important: the properties and behavior of matter at and above nuclear density.

This can be done for gravitation, the weak force, and electromagnetic forces.

This is a major hole in modern physics.

The Dense Matter Equation of State is an important Strong Force Regime

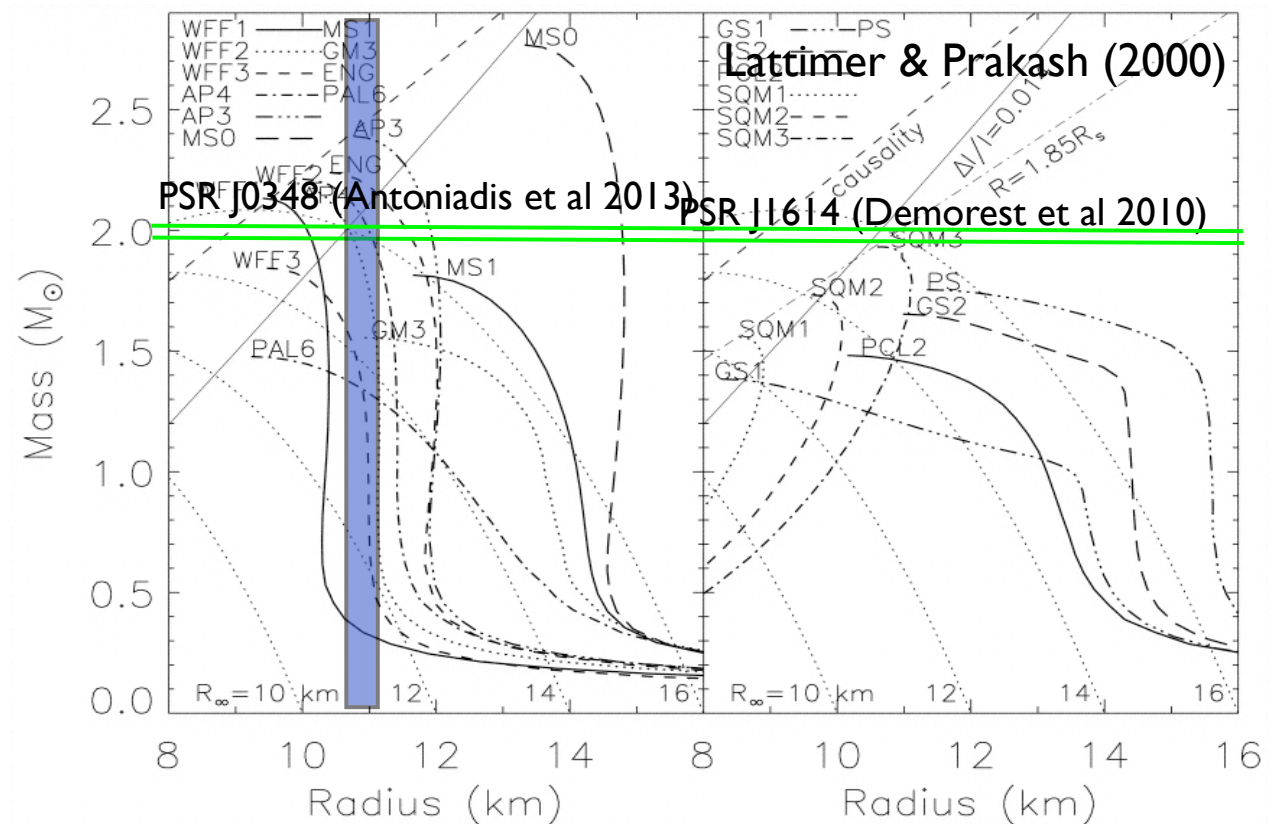
- Each different proposed dEOS produces a different mass-radius relationship for neutron stars.
- Thus, measure the mass-radius relationship of neutron stars, and you have a measurement of the dEOS.
- Precision requirement -- 5% in mass and radius, separately.
- A larger uncertainty is useless to nuclear physics.



Mass-Radius Relation from the Equation of State

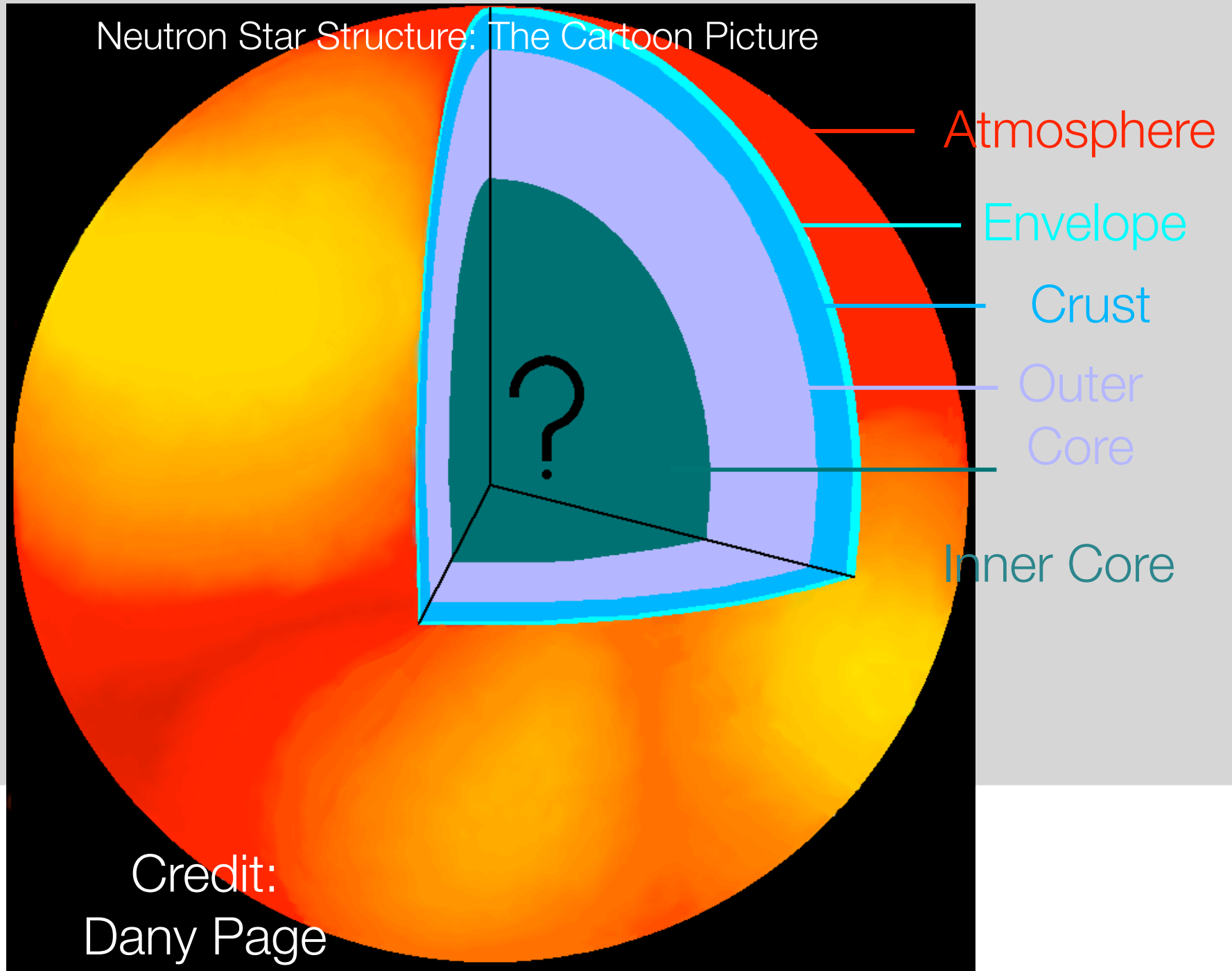
High-mass measurements prefer EOSs which produce a nearly constant radius at astrophysically interesting masses.

Measuring the Mass and Radius simultaneously is difficult.



Precision Radius Measurements (<5%) may be they key to measuring the dEOS.

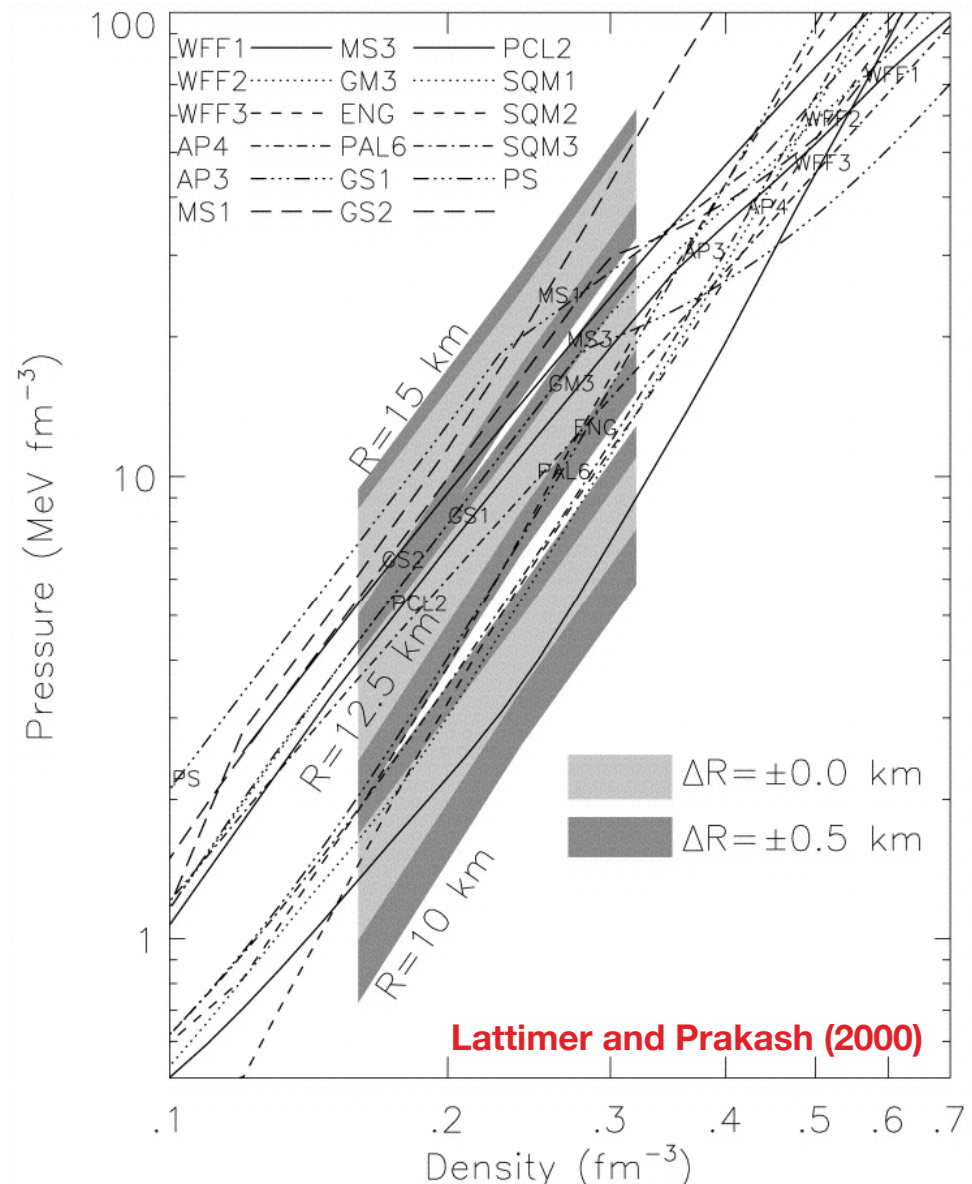
Neutron Star Structure: The Cartoon Picture



Credit:
Dany Page

Estimated Equations of State

- Different calculational (approximation) methods
- Different input physics
- Different nuclear parameters (example: nuclear compressibility as a function of fractional neutron excess).

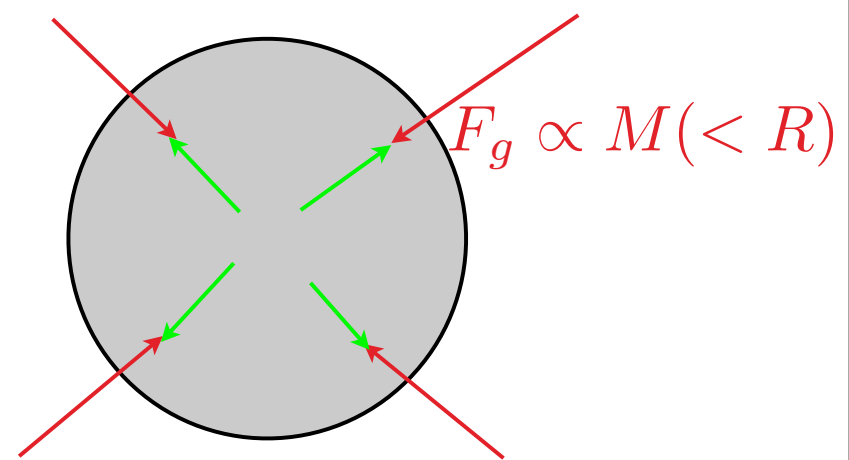


From Neutron Star Mass-Radius Relation to the Equation of State

$$P = f(\rho)$$

- Lindblom (1992) showed that each Dense Matter Equation of State maps to a unique Mass-Radius relationship for neutron stars.
- Ozel and Psaltis (2009) demonstrate how to perform the inverse problem: take the mass-radius relationship, and produce an equation of state. Only $\sim 5\text{-}7$ such objects are needed, but “with different masses”, to derive a new dense matter equation of state.
- Thus, measurement of the neutron star mass-radius relationship would implicate a unique dEOS.

Short Course:
Gravity pulls inward
Pressure Pushes Outward
Result: $R=f(M)$



Timing measurements -- which permit NS mass measurements -- are limited in precision by the stability of rotation in NS (very high) and the precision of the comparison clocks (very high).

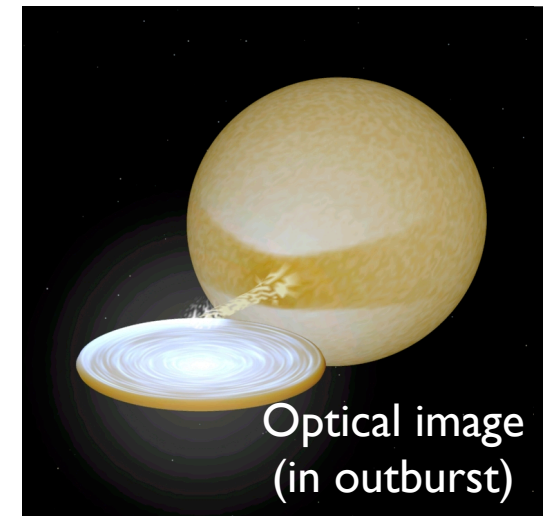
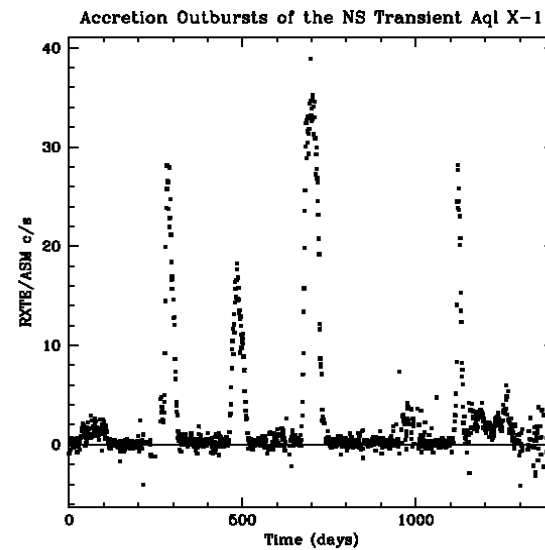
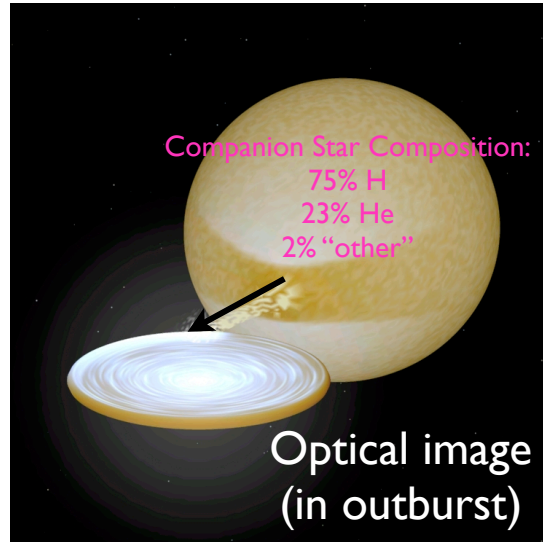
VERY LOW SYSTEMATIC UNCERTAINTIES

Result: Masses are measured to 0.0001%



Quiescent Low Mass X-ray Binaries (qLMXB)

Outburst

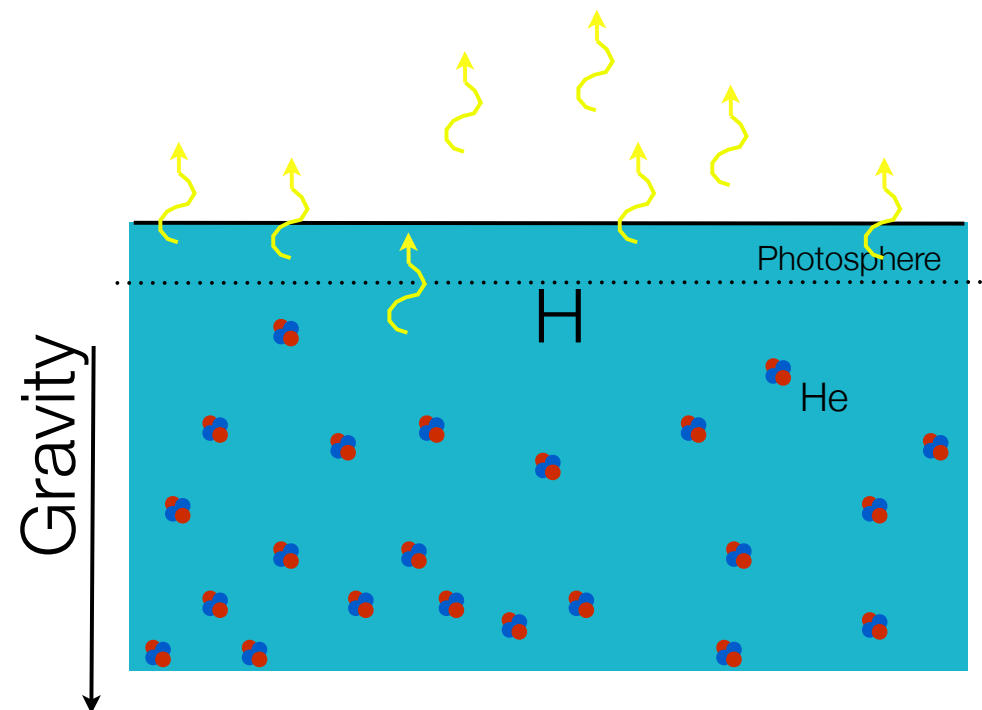


Quiescence

- Transient LMXBs in quiescence are H atmosphere neutron stars, powered by a core heated through equilibrium nuclear reactions in the crust.

qLMXBs, in this scenario, have pure Hydrogen atmospheres

- When accretion stops, the He (and heavier elements, gravitationally settle on a timescale of ~10s of seconds (like rocks in water), leaving the photosphere to be pure Hydrogen (Alcock & Illarionov 1980, Bildsten et al 1992).



Emergent Spectrum of a Neutron Star Hydrogen Atmosphere

- H atmosphere calculated Spectra are ab initio radiative transfer calculations using the Eddington equations.

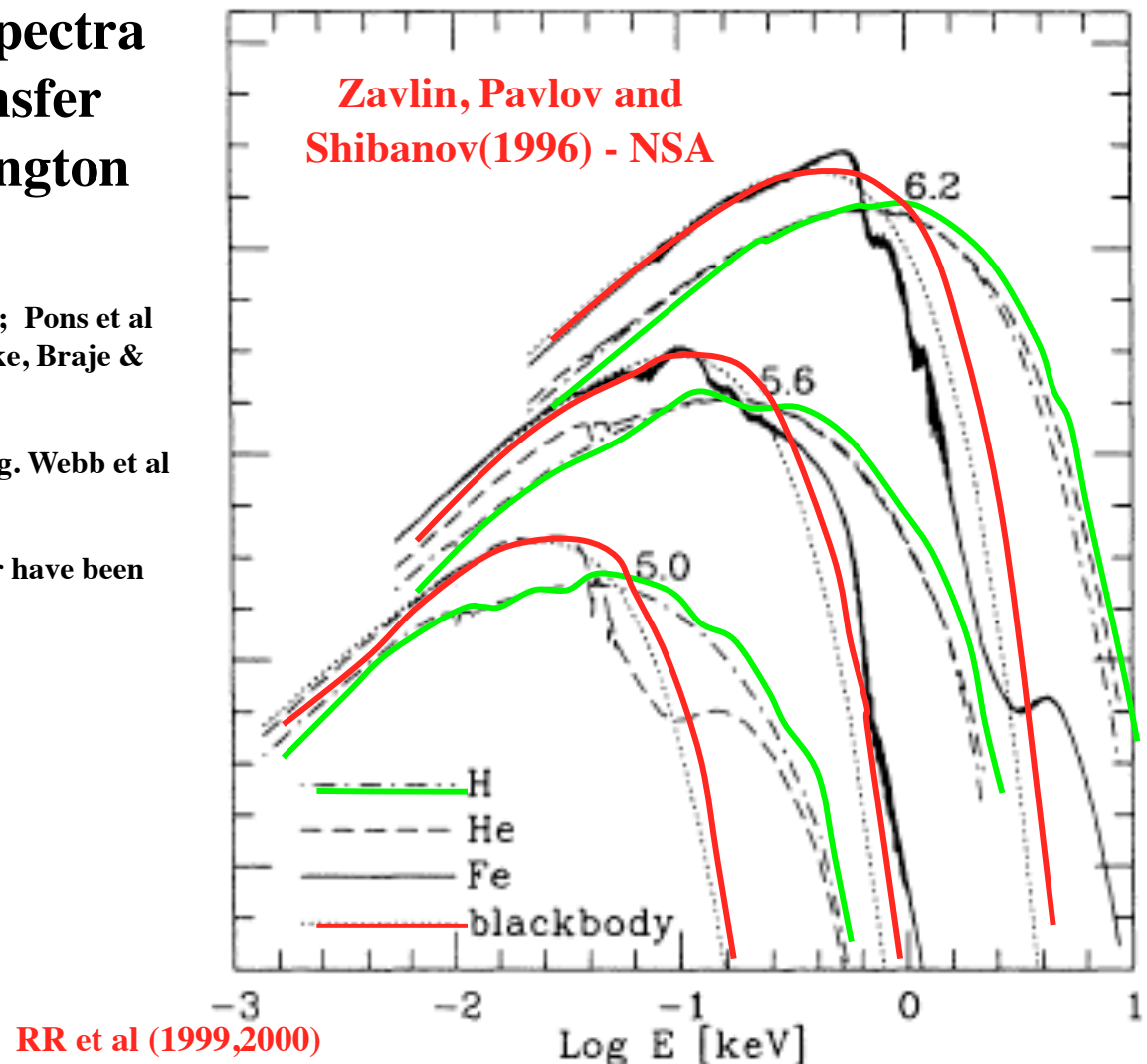
- Rajagopal and Romani (1996); Zavlin et al (1996); Pons et al (2002; Heinke et al (2006) -- NSATMOS; Gaensicke, Braje & Romani (2001); Haakonsen et al (2012)

All comparisons show consistency within ~few % (e.g. Webb et al 2007, Haakonsen 2012).

“Vetted”: X-ray spectra of Zavlin, Heinke together have been used in several dozen works.

$$F = 4\pi T_{eff,\infty}^4 \left(\frac{R_\infty}{D} \right)^2$$

$$R_\infty = \frac{R}{\sqrt{1 - \frac{2GM}{c^2 R}}}$$



Non-Equilibrium Processes in the Outer Crust

Beginning with ^{56}Fe (Haensel & Zdunik 1990, 2003)

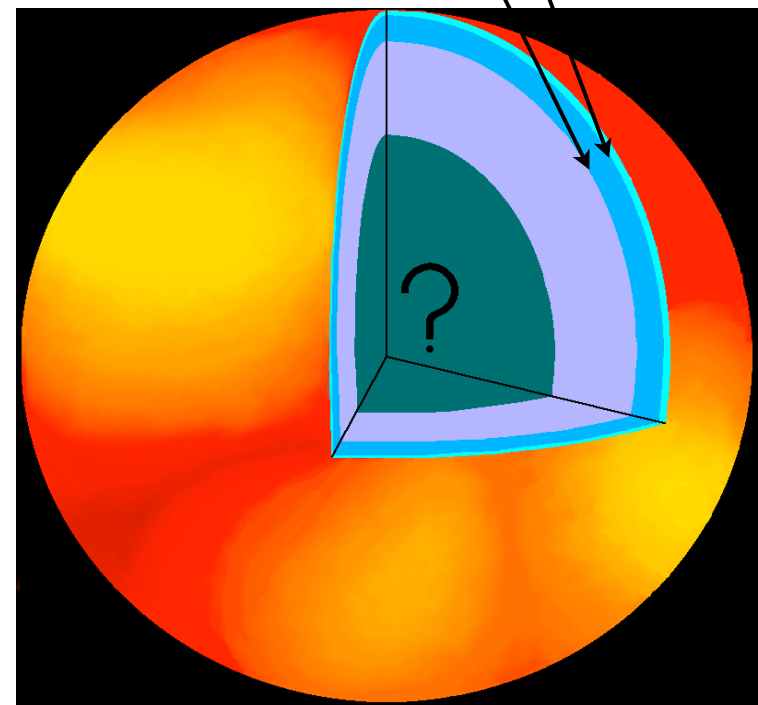
| ρ (g cm $^{-3}$) | Reaction | $\Delta\rho/\rho$ | Q (Mev/np) |
|---------------------------|---|-------------------|---------------|
| 1.5·10 ⁹ | $^{56}\text{Fe} \Rightarrow ^{56}\text{Cr} - 2\text{e}^- + 2\nu_e$ | 0.08 | 0.01 |
| 1.1·10 ¹⁰ | $^{56}\text{Cr} \Rightarrow ^{56}\text{Ti} - 2\text{e}^- + 2\nu_e$ | 0.09 | 0.01 |
| 7.8·10 ¹⁰ | $^{56}\text{Ti} \Rightarrow ^{56}\text{Ca} - 2\text{e}^- + 2\nu_e$ | 0.10 | 0.01 |
| 2.5·10 ¹⁰ | $^{56}\text{Ca} \Rightarrow ^{56}\text{Ar} - 2\text{e}^- + 2\nu_e$ | 0.11 | 0.01 |
| 6.1·10 ¹⁰ | $^{56}\text{Ar} \Rightarrow ^{52}\text{S} + 4\text{n} - 2\text{e}^- + 2\nu_e$ | 0.12 | 0.01 |

Non-Equilibrium Processes in the Inner Crust

| ρ (g cm $^{-3}$) | Reaction | X_n | Q (Mev/np) |
|---------------------------|--|-------|---------------|
| 9.1·10 ¹¹ | $^{52}\text{S} \Rightarrow ^{46}\text{Si} + 6\text{n} - 2\text{e}^- + 2\nu_e$ | 0.07 | 0.09 |
| 1.1·10 ¹² | $^{46}\text{Si} \Rightarrow ^{40}\text{Mg} + 6\text{n} - 2\text{e}^- + 2\nu_e$ | 0.07 | 0.09 |
| 1.5·10 ¹² | $^{40}\text{Mg} \Rightarrow ^{34}\text{Ne} + 6\text{n} - 2\text{e}^- + 2\nu_e$ | | |
| | $^{34}\text{Ne} + ^{34}\text{Ne} \Rightarrow ^{68}\text{Ca}$ | 0.29 | 0.47 |
| 1.8·10 ¹² | $^{68}\text{Ca} \Rightarrow ^{62}\text{Ar} + 6\text{n} - 2\text{e}^- + 2\nu_e$ | 0.39 | 0.05 |
| 2.1·10 ¹² | $^{62}\text{Ar} \Rightarrow ^{56}\text{S} + 6\text{n} - 2\text{e}^- + 2\nu_e$ | 0.45 | 0.05 |
| 2.6·10 ¹² | $^{56}\text{S} \Rightarrow ^{50}\text{Si} + 6\text{n} - 2\text{e}^- + 2\nu_e$ | 0.50 | 0.06 |
| 3.3·10 ¹² | $^{50}\text{Si} \Rightarrow ^{44}\text{Mg} + 6\text{n} - 2\text{e}^- + 2\nu_e$ | 0.55 | 0.07 |
| 4.4·10 ¹² | $^{44}\text{Mg} \Rightarrow ^{36}\text{Ne} + 6\text{n} - 2\text{e}^- + 2\nu_e$ | | |
| | $^{36}\text{Ne} + ^{36}\text{Ne} \Rightarrow ^{72}\text{Ca}$ | | |
| | $^{68}\text{Ca} \Rightarrow ^{62}\text{Ar} + 6\text{n} - 2\text{e}^- + 2\nu_e$ | 0.61 | 0.28 |
| 5.8·10 ¹² | $^{62}\text{Ar} \Rightarrow ^{60}\text{S} + 6\text{n} - 2\text{e}^- + 2\nu_e$ | 0.70 | 0.02 |
| 7.0·10 ¹² | $^{60}\text{S} \Rightarrow ^{54}\text{Si} + 6\text{n} - 2\text{e}^- + 2\nu_e$ | 0.73 | 0.02 |
| 9.0·10 ¹² | $^{54}\text{Si} \Rightarrow ^{48}\text{Mg} + 6\text{n} - 2\text{e}^- + 2\nu_e$ | 0.76 | 0.03 |
| 1.1·10 ¹³ | $^{48}\text{Mg} + ^{48}\text{Mg} \Rightarrow ^{96}\text{Cr}$ | 0.79 | 0.11 |
| 1.1·10 ¹³ | $^{96}\text{Cr} \Rightarrow ^{88}\text{Ti} + 8\text{n} - 2\text{e}^- + 2\nu_e$ | 0.80 | 0.01 |

Deep Crustal Heating

Begins Here
Ends Here



1.47 Mev per np

Brown, Bildsten & RR (1998)

Assumptions -- the systematic uncertainties.

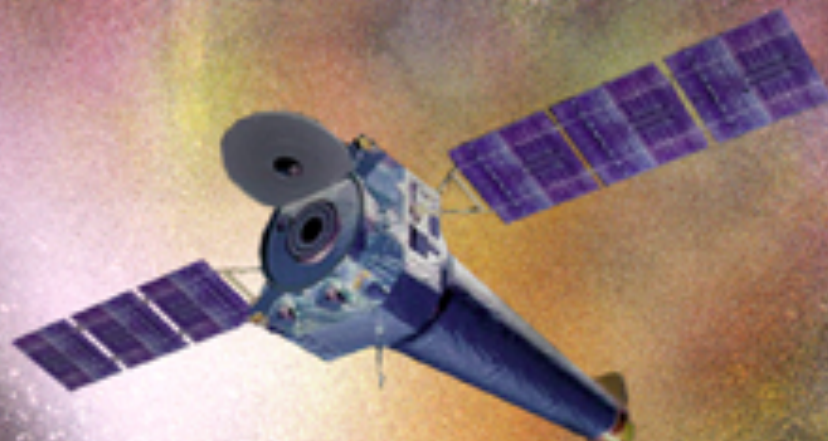
- **H atmosphere neutron stars.** Expected from a Hydrogen companion LMXB; can be supported through optical observations of a H companion.
- **Low B-field ($<10^{10}$ G) neutron stars.** This is true for ‘standard’ LMXBs as a class, but difficult to prove on a case-by-case basis.
- **Emitting isotropically.** Occurs naturally when powered by a hot core.
- **Non-Rotating neutron stars.** qLMXBs are observed to rotate at 100-600 Hz. This can be a significant fraction of the speed of light. Doppler boosting and deviation from NS spheroidal geometry are not included in emission models. *These effects should be calculated, but have not yet been.*

If you don't like these assumptions: “We find the assumptions not strongly supported and therefore ignore this result.”

Instruments for measurements of qLMXBs

Chandra X-ray Observatory

- Launched 1999 (NASA)
 - 1" resolution



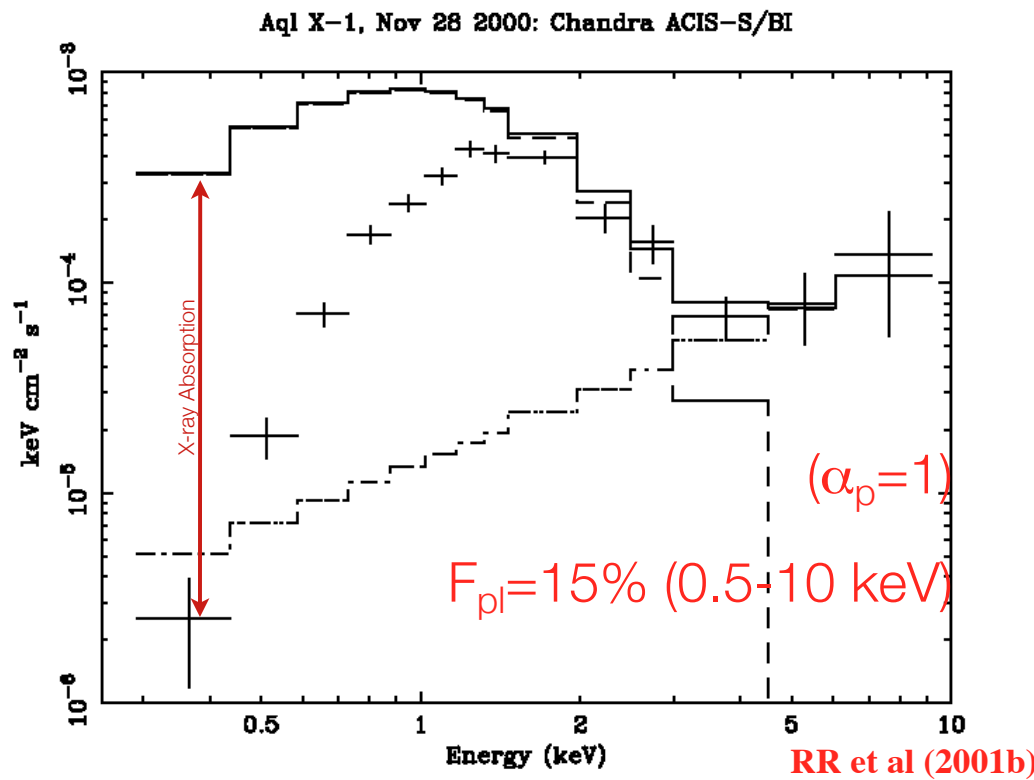
XMM/Newton

- Launched 1999 (ESA)
- 6" resolution
- ~4x area of Chandra.

Every photon is time tagged (~ 1 sec), with its energy measured ($E/\Delta E = 10$) with full resolution imaging.



Aql X-1 with Chandra -- Field Source



$R_\infty (\text{d}/5 \text{ kpc})$

13^{+5}_{-4} km

$kT_{\text{eff},\infty}$

$135^{+18}_{-12} \text{ eV}$

N_{H}

$(1e20 \text{ cm}^{-2})$

35^{+8}_{-7}

The LMXB Factories: Globular Clusters

- GCs : overproduce LMXBs by 1000x vs. field stars
- Many have accurate distances measured.

qLMXBs can be identified by their soft X-ray spectra, and confirmed with optical counterparts.

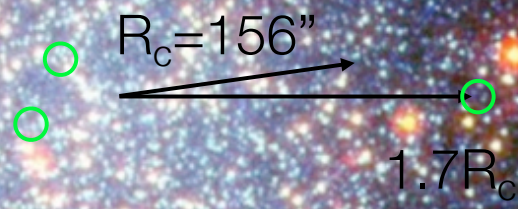


| NGC | D (kpc) | +/- (%) |
|------|---------|---------|
| 104 | 5.13 | 4 |
| 288 | 9.77 | 3 |
| 362 | 10.0 | 3 |
| 4590 | 11.22 | 3 |
| 5904 | 8.28 | 3 |
| 7099 | 9.46 | 2 |
| 6025 | 7.73 | 2 |
| 6341 | 8.79 | 3 |
| 6752 | 4.61 | 2 |

Carretta et al (2000)

NGC 5139 (Omega Cen)

qLMXBs can be identified by their soft X-ray spectra, and confirmed with optical counterparts.



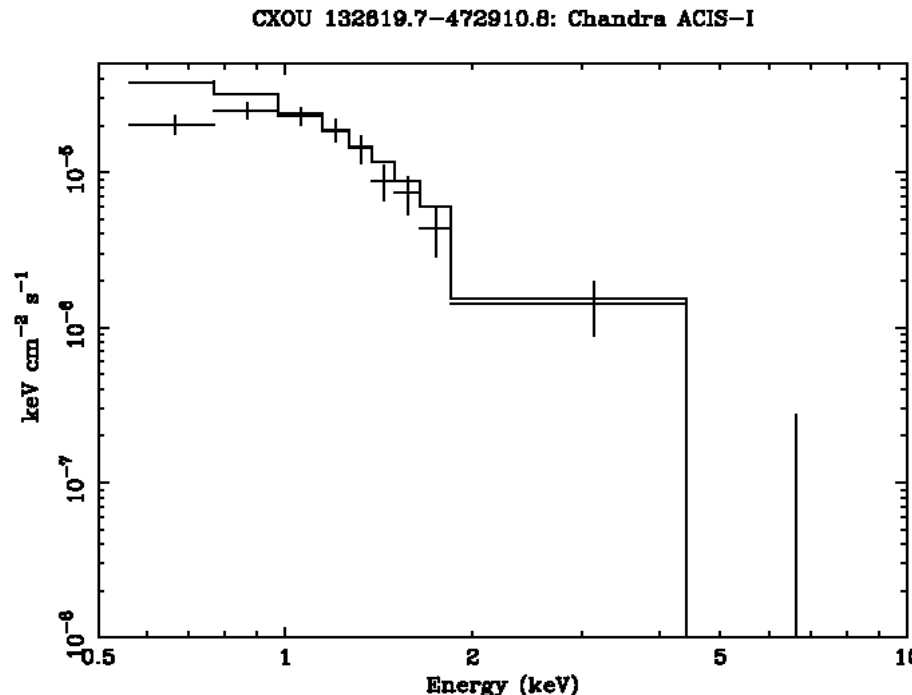
The identified optical counterpart demonstrates unequivocally the X-ray source is a qLMXB.

An X-ray source well outside the cluster core
Spitzer (Infrared)

NGC 5139 (Omega Cen)

X-ray Spectrum is inconsistent with any other type of known GC source (pulsars, CVs, coronal sources).

Full confirmation as LMXB requires Hubble photometry



R_∞ (d/5 kpc)

$kT_{\text{eff},\infty}$

N_H
(1e20 cm⁻²)

14.3 ± 2.1 km

66^{+4}_{-5} eV

(9)

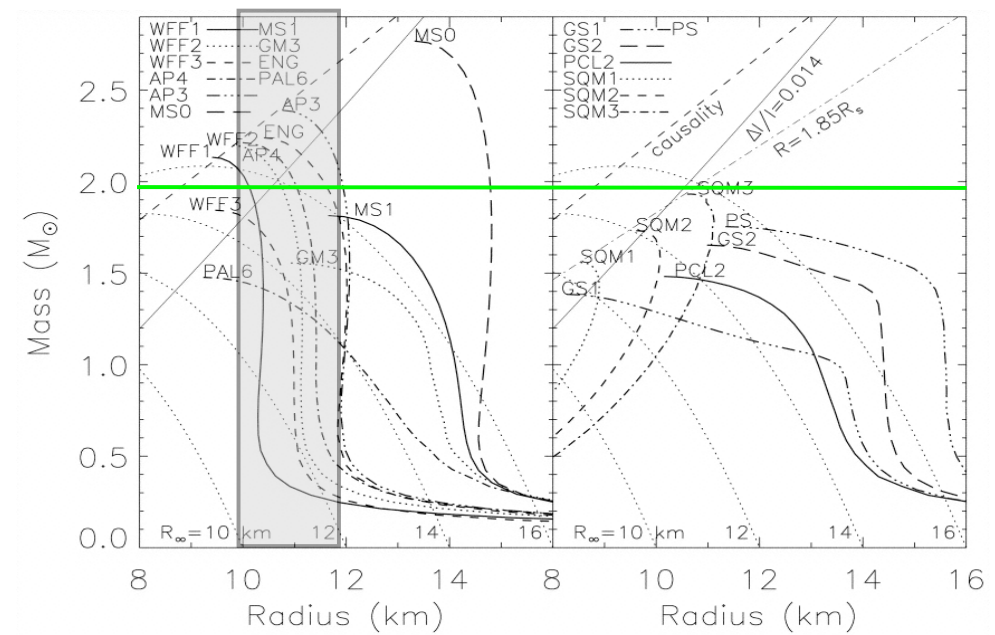
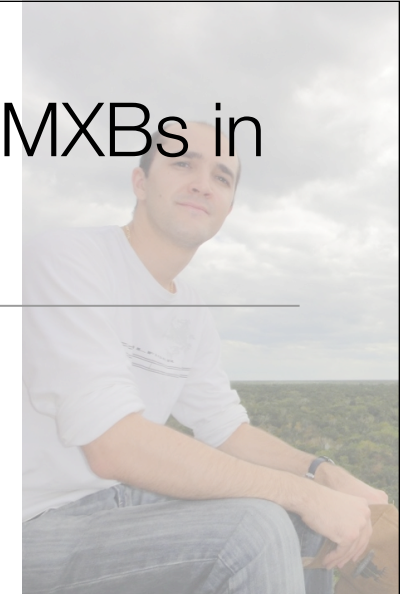
RR et al (2002)

All qLMXBs used in this work were previously identified and analysed, with resulting R published.

| Name | kT_eff(infty) (eV) | NH | Fx (10^{-13} cgsflux) | Band (keV) | Ref. | R(infty) |
|----------------|-----------------------|----------|-----------------------------|---------------|--|------------|
| 47 Tuc X7 | 105(5) | 0.04(2) | 5.3 | 0.5-10 | Heinke et al (2006) | < 5" |
| 47 Tuc X5 | 100(20) | 0.09(7) | 4.3 | 0.5-10 | Heinke et al (2003) | < 5" |
| M28 | 90(+30-10) | 0.26(4) | 3.4 | 0.5-8 | Becker et al (2003) | <5" |
| NGC 6304 X9 | 115(20) | [0.266] | 1.5 | 0.5-10 | Guillot et al (2009) | +++ |
| NGC 6304 X4 | 120(20) | [0.266] | 1.1 | 0.5-10 | Guillot et al (2009) | <15" |
| NGC 6397 (U24) | 74(18) | 0.1-0.26 | 1.06 | 0.5-2.5 | Grindlay et al (2001) | < 15" |
| M13 | 76(3) | [0.011] | 1.03 | 0.1-5 | Gendre et al (2003) | DONE |
| NGC 3201 X16 | 170 (50) | [0.14] | 1.0 | 0.6-6 | Webb et al (2006) | Data taken |
| NGC 6553 X9 | 100 (20) | [0.35] | 1.0 | 0.5-10 | Guillot et al (in prep) | +++ |
| Omega Cen | 67(2) | 0.09(3) | 0.95 | 0.1-5 | Rutledge et al (2002), Gendre et al (2003) | DONE |
| NGC 6637 X3 | 100 (40) | [0.11] | 0.84 | 0.5-10 | Guillot et al (in prep) | +++ |
| M30 A-1 | 94(15) | 0.03(1) | 0.73 | 0.5-10 | Lugger (2007) | <10" |
| NGC 6553 X3 | 127(+7-45) | [0.35] | 0.65 | 0.5-10 | Guillot et al (in prep) | <: 5" |
| NGC 6304 X5 | 70(25) | [0.266] | 0.32 | 0.5-10 | Guillot et al (2008) | +++ |
| NGC 6553 x35 | 88 (60) | [0.35] | 0.3 | 0.5-10 | Guillot et al (in prep) | +++ |
| NGC 2808 C2 | -- | 0.86 | 0.24 | -- | Servillat et al (2008) | <15" |
| M80 CX2 | 82(2) | 0.09(2) | 0.23 | 0.5-6 | Heinke et al (2003) | <5" |
| M80 CX6 | 76(6) | 0.22(7) | 0.07 | 0.5-6 | Heinke et al (2003) | <15" |

Measuring the Radius of Neutron Stars from qLMXBs in Globular Clusters

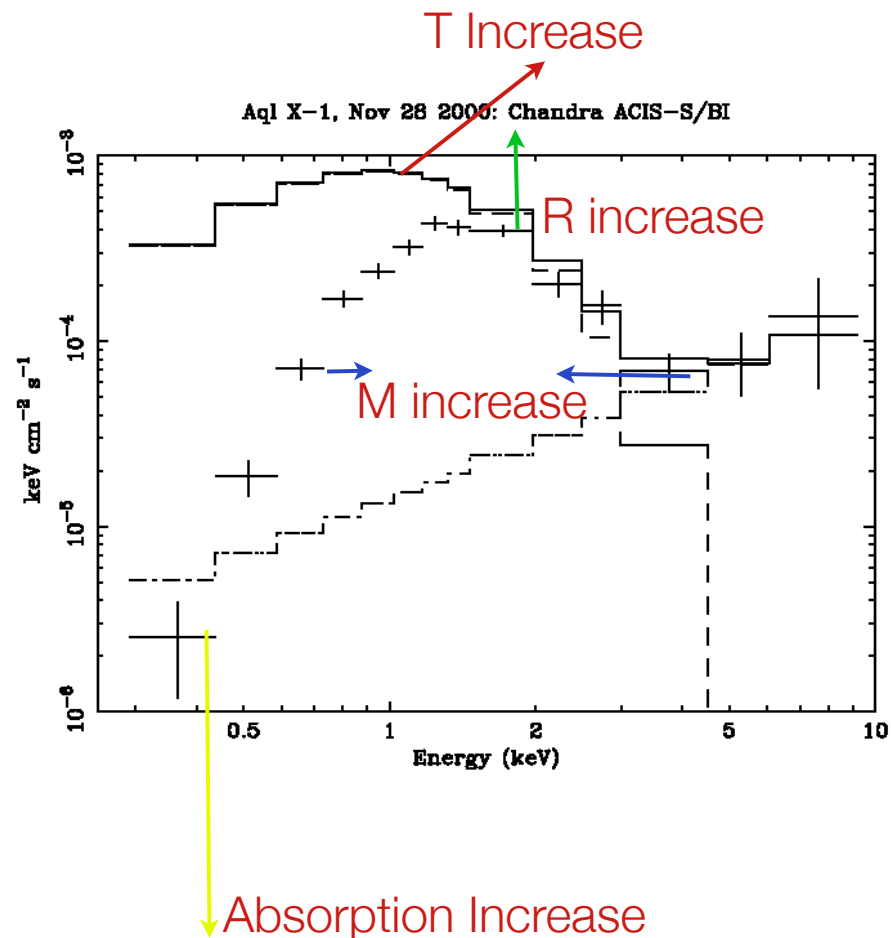
- The 2.0 solar mass neutron stars favor hadronic dEOSs over quark and phase-transition dEOSs. **These have the property of a quasi-constant neutron star radius.**
- Analysis goal: **Using all suitable qLMXB X-ray data sets of targets (there are five) provide the most reliable neutron star radius measurement possible.**
- Assume the radius of neutron stars is **quasi-constant** (a constant, at astrophysically important masses, within measurement error).
- Perform a Markoff-Chain-Monte-Carlo (MCMC) and include all known uncertainties and use conservative assumptions.



All previous EoS work treated measurements of each NS independently, and combined their statistics inefficiently.

$$\frac{\partial \chi^2}{\partial(p1)\partial(p2)} = \begin{pmatrix} \text{Source 1} & & \text{Source 2} \\ R_1 & M_1 & T_1 & N_{H,1} & R_2 & M_2 & T_2 & N_{H,2} \end{pmatrix} \begin{pmatrix} R_1 \\ M_1 \\ T_1 \\ N_{H,1} \\ R_2 \\ M_2 \\ T_2 \\ N_{H,2} \end{pmatrix}$$

$$\begin{pmatrix} \frac{1}{\sigma_{R_1}^2} & a_{1,2} & a_{1,3} & a_{1,4} & 0 & 0 & 0 & 0 \\ a_{2,1} & \frac{1}{\sigma_{M_1}^2} & a_{2,3} & a_{2,4} & 0 & 0 & 0 & 0 \\ a_{3,1} & a_{3,2} & \frac{1}{\sigma_{T_1}^2} & a_{3,4} & 0 & 0 & 0 & 0 \\ a_{4,1} & a_{4,2} & a_{4,3} & \frac{1}{\sigma_{N_{H,1}}^2} & 0 & 0 & 0 & 0 \\ 0 & 0 & 0 & 0 & \frac{1}{\sigma_{R_2}^2} & a_{5,6} & a_{5,7} & a_{5,8} \\ 0 & 0 & 0 & 0 & a_{6,5} & \frac{1}{\sigma_{M_2}^2} & a_{6,7} & a_{6,8} \\ 0 & 0 & 0 & 0 & a_{7,5} & a_{7,6} & \frac{1}{\sigma_{T_2}^2} & a_{7,8} \\ 0 & 0 & 0 & 0 & a_{8,5} & a_{8,6} & a_{8,7} & \frac{1}{\sigma_{N_{H,2}}^2} \end{pmatrix}$$



“Joint Fits” - the major difference from previous work

$$\frac{\partial \chi^2}{\partial(p1)\partial(p2)} = \left(\begin{array}{cccc|cccc} & \text{Source 1} & & & \text{Source 2} & & & \\ \textcolor{red}{R} & M_1 & T_1 & N_{H,1} & \textcolor{blue}{R} & M_2 & T_2 & N_{H,2} \\ \hline \frac{1}{\sigma_R^2} & a_{1,2} & a_{1,3} & a_{1,4} & \frac{1}{\sigma_R^2} & a_{1,6} & a_{1,7} & a_{1,8} \\ a_{2,1} & \frac{1}{\sigma_{M_1}^2} & a_{2,3} & a_{2,4} & a_{2,5} & \frac{1}{\sigma_{M_1, M_2}^2} & a_{2,7} & a_{2,8} \\ a_{3,1} & a_{3,2} & \frac{1}{\sigma_{T_1}^2} & a_{3,4} & a_{3,5} & a_{3,6} & \frac{1}{\sigma_{T_1, T_2}^2} & a_{3,8} \\ a_{4,1} & a_{4,2} & a_{4,3} & \frac{1}{\sigma_{N_{H1}}^2} & a_{4,5} & a_{4,6} & a_{4,7} & \frac{1}{\sigma_{N_{H1}, N_{H2}}^2} \\ \frac{1}{\sigma_R^2} & a_{5,2} & a_{5,3} & a_{5,4} & \frac{1}{\sigma_R^2} & a_{5,6} & a_{5,7} & a_{5,8} \\ a_{6,1} & \frac{1}{\sigma_{M_2, M_1}^2} & a_{6,3} & a_{6,4} & a_{6,5} & \frac{1}{\sigma_{M_2}^2} & a_{6,7} & a_{6,8} \\ a_{7,1} & a_{7,2} & \frac{1}{\sigma_{T_2, T_1}^2} & a_{7,4} & a_{7,5} & a_{7,6} & \frac{1}{\sigma_{T_2}^2} & a_{7,8} \\ a_{8,1} & a_{8,2} & a_{8,3} & \frac{1}{\sigma_{N_{H2}, N_{H1}}^2} & a_{8,5} & a_{8,6} & a_{8,7} & \frac{1}{\sigma_{N_{H2}}^2} \end{array} \right) \begin{matrix} R_1 \\ M_1 \\ T_1 \\ N_{H,1} \\ R_2 \\ M_2 \\ T_2 \\ N_{H,2} \end{matrix}$$

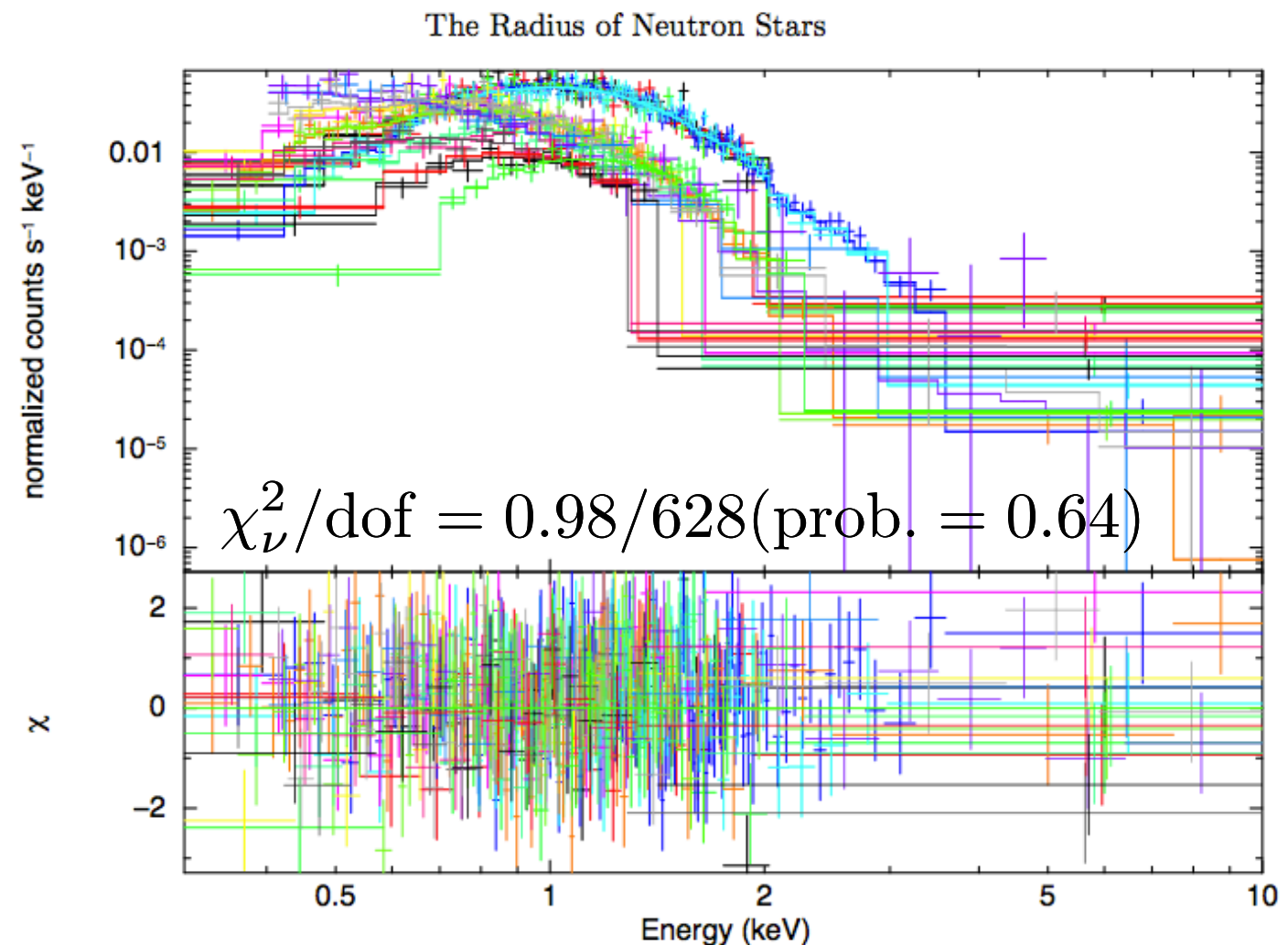
Every parameter (M, R, T, N_H) of all five sources affects every other parameter of every source

$$\frac{S}{N} \propto \frac{N^2(\# \text{ of Source Matrix Elements})}{N(\# \text{ of sources})} = N$$

In comparison to using the sources “independently”, its as if we have 25 sources, instead of 5 sources.

Best H atmosphere (+ PL) spectral fit of all 5 qLMXBs

- This model is a statistically acceptable fit to the X-ray spectral data. This is an a posteriori confirmation that the data are consistent with our assumptions.
- After finding the best fit a MCMC method was used to find the uncertainty regions for all parameters - - - the Radius, Mass, Temperature, absorption, distance, and power-law normalization.



Guillot et al (2013)

NH free, D gaussian bayesian priors, PL included.

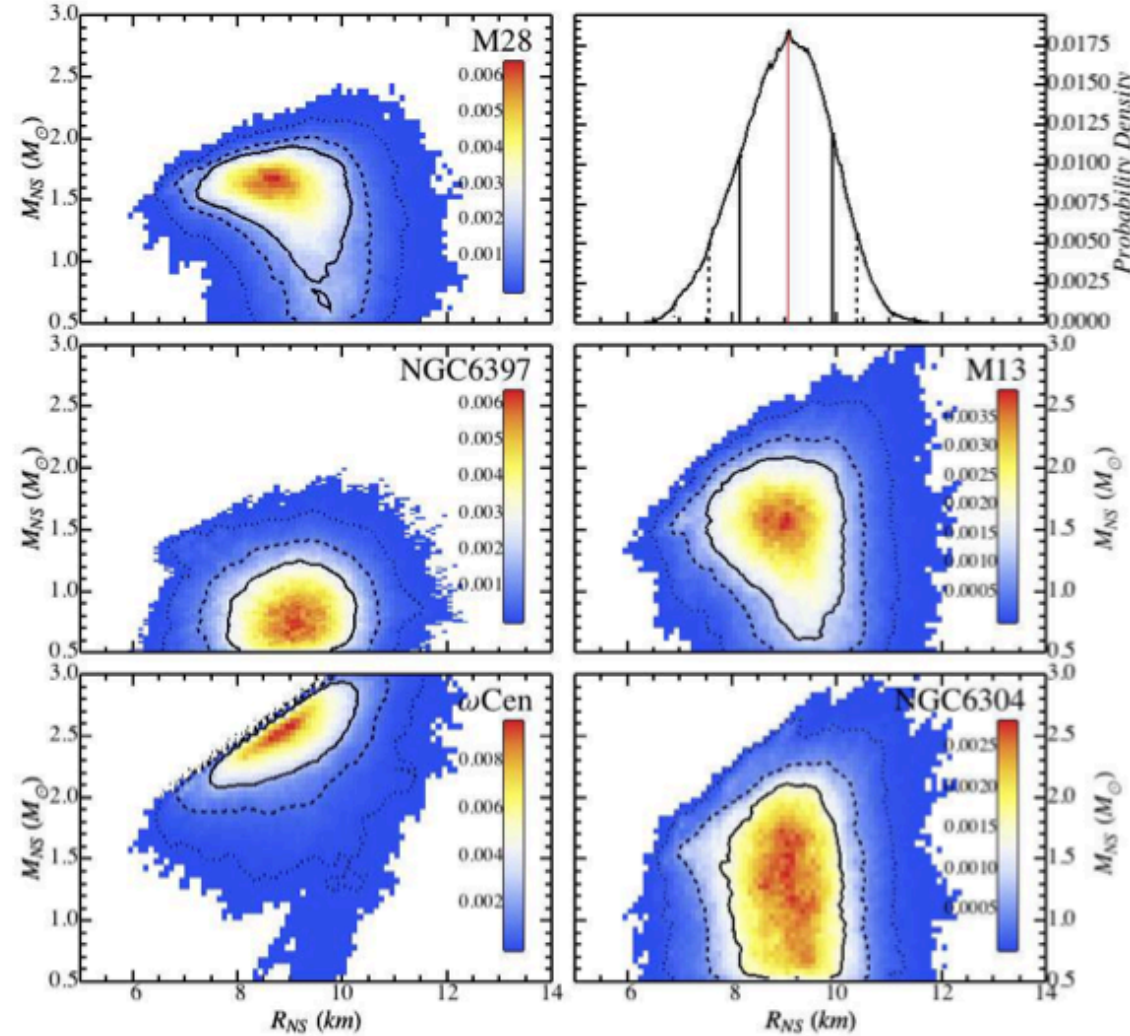
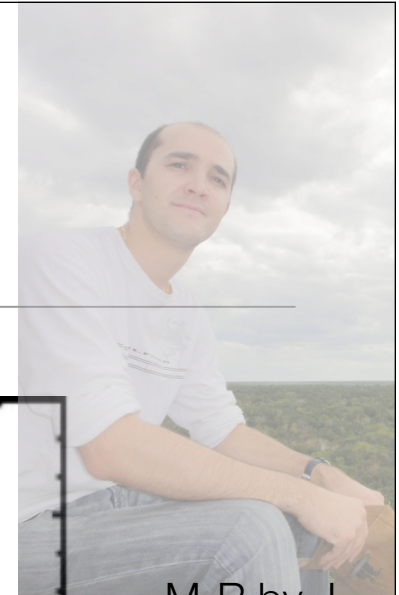
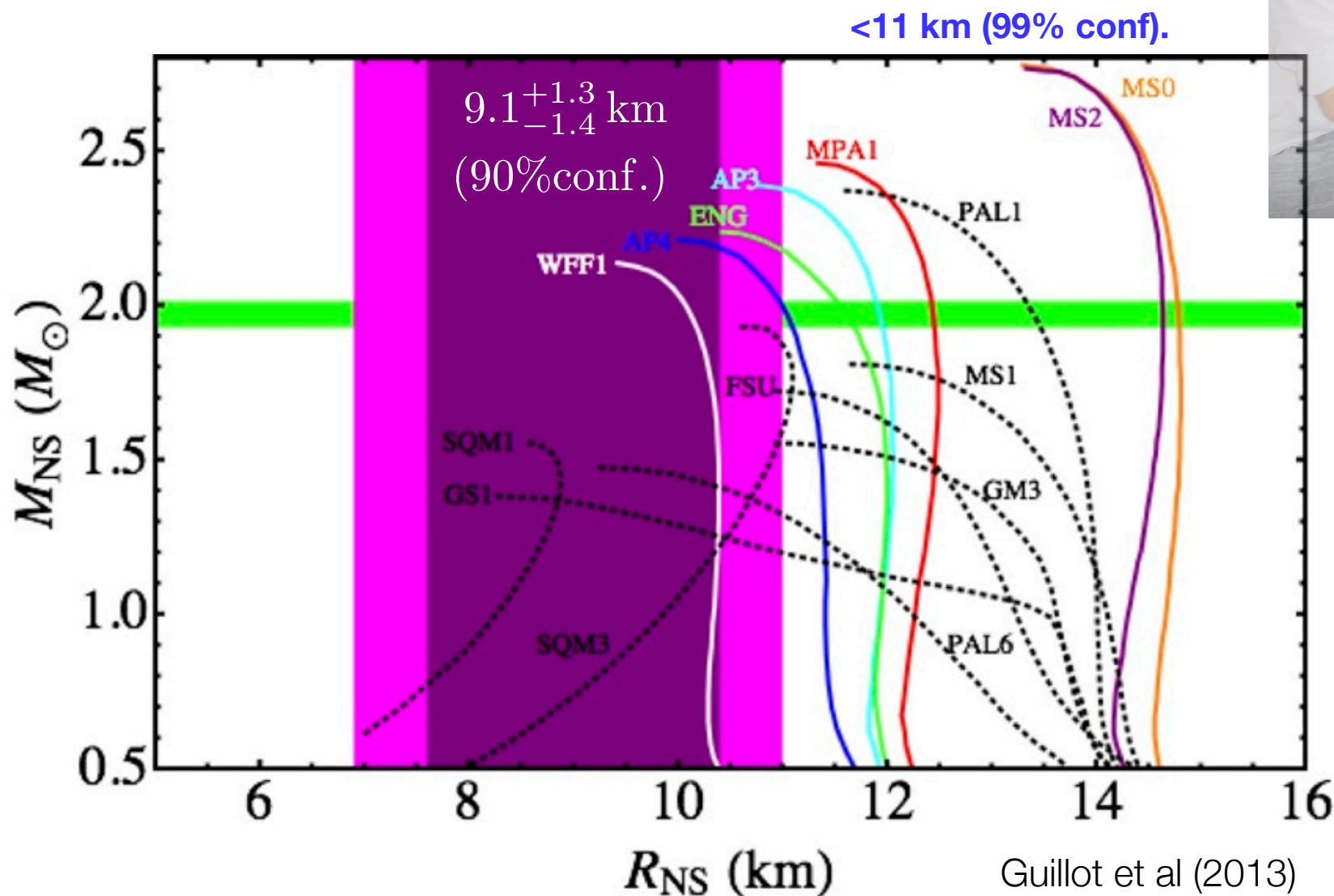


FIG. 15.— Figure similar to Figure 9 corresponding to Run #7. Here, all the possible assumptions have been relaxed to obtain a R_{NS} measurement the least affected by systematic uncertainties. The N_H parameters are left free; and Gaussian Bayesian priors and PL components are included. This results in an R_{NS} measurement: $R_{NS} = 9.1^{+1.3}_{-1.5}$ km

Guillot et al (2013)

The Neutron Star Radius



M-R by J.
Lattimer

WFF1=
Wiring, Fiks
and Fabrocini
(1988)